Molecular cloning and transient expression in COS7 cells of a novel human PDE4B cAMP-specific phosphodiesterase, HSPDE4B3

Elaine HUSTON*, Simon LUMB†, Annette RUSSELL†, Cath CATTERALL†, Annette H. ROSS*, Michael R. STEELE‡§, Graeme B. BOLGER‡§, Martin J. PERRY†, Raymond J. OWENS† and Miles D. HOUSLAY*[1]

*Division of Biochemistry and Molecular Biology, Wolfson Building, University of Glasgow, Glasgow G12 8QQ, Scotland, U.K., †CellTech Therapeutics Ltd., 216 Bath Road, Slough, Berks. SL1 4EN, U.K., ‡Department of Veterans Affairs Medical Center, 151M, and Huntsman Cancer Institute, Department of Oncologic Sciences and §Department of Medicine (Hematology/Oncology), University of Utah Health Sciences Center, 500 Foothill Blvd., Salt Lake City, UT 84148, U.S.A.

5′-Rapid amplification of cDNA ends, done on poly(A)$^+$ RNA from human U87 cells, was used to identify 420 bp of novel 5′ sequence of a PDE4B cAMP-specific phosphodiesterase (PDE). This identified an open reading frame encoding a putative 721-residue 'long-form' PDE4B splice variant, which we term HSPDE4B3. HSPDE4B3 differs from the two known PDE4B forms by virtue of its unique 79-residue N-terminal region, compared with the unique N-terminal regions of 94 and 39 residues found in HSPDE4B1 and HSPDE4B2 respectively. In transfected COS7 cells the two long forms, HSPDE4B1 and HSPDE4B3, had molecular masses of approx. 104 and approx. 103 kDa respectively. Expressed in COS-7 cells, the three HSPDE4B isoforms were found in the high-speed supernatant (cytosol) fraction as well as both the high-speed pellet (P2) and low-speed pellet (P1) fractions. All isoforms showed similar K_m values for cAMP hydrolysis (1.5–2.6 μM). The maximal activities of the soluble cytosolic activity of the two long forms were very similar, whereas that of the short form, HSPDE4B2, was approx. 4-fold higher. Particulate-associated HSPDE4B1 and HSPDE4B2 were less active (approx. 40 %) than their cytosol forms, whereas particulate HSPDE4B3 was similar in activity to its cytosolic form. Particulate and cytosolic forms of HSPDE4B1 and HSPDE4B3 were similarly inhibited by rolipram {4-[3-(cyclopentoxyl)-4-methoxyphenyl]-2-pyrrolidone}, the selective inhibitor of PDE4 (IC_{50} 0.05–0.1 μM), whereas particulate-associated HSPDE4B2 was profoundly (approx. 10-fold) more sensitive (IC_{50} 0.02 μM) to rolipram inhibition than its cytosolic form (IC_{50} 0.2 μM). The various particulate-associated HSPDE4B isoforms showed very different susceptibilities to solubilization with the detergent Triton X-100 and high NaCl concentration. A novel cDNA, called pRPDE74, was obtained by screening a rat olfactory lobe cDNA library. This contained an open reading frame encoding a 721-residue protein that showed approx. 96 % amino acid identity with HSPDE4B3 and is proposed to reflect the rat homologue of this human enzyme and is thus called RNPDE4B3. Alternative splicing of mRNA generated from both the human and rat PDE4B genes produces long and short splice variants that have unique N-terminal splice regions. It is suggested that these alternatively spliced regions determine changes in the maximal catalytic activity of the isoforms, their susceptibility to inhibition by rolipram and mode of interaction with particulate fractions.

INTRODUCTION

Inactivation of the second messenger cAMP is achieved through the action of members of a large family of cyclic nucleotide phosphodiesterases (PDEs) [1–9]. These are the products of multiple genes, producing enzymes having markedly different regulatory characteristics. The cell-specific expression of PDE isoforms might thus allow particular cell types to tailor individually the control of cAMP signalling as well as determining the intracellular compartmentalization of cAMP [10].

The cAMP-specific PDE4 family (a rolipram {4-[3-(cyclopentoxyl)-4-methoxyphenyl]-2-pyrrolidone}-inhibited PDE subfamily) was first recognized as a distinct entity after the use of both biochemical separation procedures and compounds such as rolipram, which served as specific and selective inhibitors of this enzyme family [11] and have potential therapeutic use as anti-inflammatory agents [12,13] and anti-depressants [14]. Sensitivity to rolipram inhibition also permitted the categorization, as PDE4 family members, of various previously isolated and purified cAMP-specific PDE species [15–17].

The *Drosophila melanogaster dunc* PDE, which is also a cAMP-specific enzyme, provided the first PDE cDNA to be isolated and then was used to effect the cloning of a family of PDE4 forms from rodents [18,19]. Subsequently, human PDE4 cDNA species were isolated [20–25]. In rodents and man four genes encode PDE4 isoforms [26–28], with each of these seeming to produce multiple protein products [3,6]. These isoforms are produced through alternative mRNA splicing and, with one recorded exception noted for the product of the human PDE4A gene [26,29], exclusively take the form of 5′ domain swaps yielding isoforms with distinct N-terminal regions. From analyses [30–38] done on PDE4A isoforms it has been suggested that these N-terminal domains can confer distinct properties on isoforms, identified as governing intracellular targeting to distinct membrane and cytoskeletal locations, interaction with specific proteins, such as SH3-containing species, and regulating the enzyme V_{max}.

Abbreviations used: DMEM, Dulbecco's modified Eagle's medium; HSPDE4B1, a long-form human PDE4B; HSPDE4B2, a short-form human PDE4B; HSPDE4B3, a long-form human PDE4B; ORF, open reading frame; plasmids pde4 and rpde18 are PDE4B2 forms (GenBank accession numbers M25350, M28413 and L27058); PDE, cAMP phosphodiesterase; PDE4, rolipram-inhibited PDE subfamily; RACE, rapid amplification of cDNA ends; RNPDE4B3, a long-form rat PDE4B; rolipram, 4-[3-(cyclopentoxyl)-4-methoxyphenyl]-2-pyrrolidone; RT–PCR, reverse transcriptase–PCR; UCR, upstream conserved region.

[1] To whom correspondence should be addressed.

The nucleotide sequence results reported here (HSPDE4B1, HSPDE4B2, HSPDE4B3 and RNPDE4B3) will appear in DDBJ, EMBL and GenBank Nucleotide Sequence Databases under the accession numbers L20966; M97515, L20971 and L12686; U85048; and U95748 respectively.

Additionally, for the PDE4D family it has been shown [24,39,40] that the unique N-terminal region of PDE4D3 can confer susceptibility to phosphorylation and activation of this isoform by protein kinase A.

The first PDE4B cDNA to be isolated [41] was from rat and was called DPD (GenBank accession number J04563). However, this particular cDNA (RNPDE4B1) is now known to represent an N-terminally truncated form, as the full-length human homologue of this species (TM72; HSPDE4B1A; GenBank accession number L20966) has been identified [20]. A further rat PDE4B splice variant, called pde4, was isolated by homology cloning [19], with the human homologue of this form, RNPDE4B2, having been identified subsequently [20,22,42].

Here we describe the molecular cloning, by rapid amplification of cDNA ends (RACE), of a novel human HSPDE4B splice variant, which we term PDE4B3. We also report the molecular cloning of its rat homologue, called RNPDE4B3, by screening of rat olfactory lobe cDNA library. For the first time the properties of each of the full-length human PDE4B isoforms are analysed when expressed in mammalian cells with the monkey kidney epithelial COS7 cell line.

MATERIALS AND METHODS

Materials

Restriction enzymes, Dulbecco's modified Eagle's medium (DMEM) and foetal calf serum were from Gibco/BRL (Paisley, Scotland, U.K.). Tris, Hepes, DEAE-dextran (molecular mass 500 kDa), cytochalasin B, benzamidine hydrochloride, PMSF, aprotinin, pepstatin A, antipain, EDTA, EGTA, cAMP, cGMP, Dowex 1X8-400 (chloride form, 200–400 mesh), 3-isobutyl-1-methylxanthine, snake (*Ophiophagus hannah*) venom, PBS, isopropyl β-D-thiogalactoside, ampicillin, glutathione and bovine brain calmodulin were from Sigma Chemical Co. (Poole, Dorset, U.K.). Nuserum was from Collaborative Biomedical Products (London, U.K.). [^{3}H]cAMP and [^{3}H]cGMP were from Amersham International (Little Chalfont, Bucks., U.K.). Leupeptin was from Peptide Research Foundation (distributed by Scientific Marketing Associates, London, U.K.). Dithiothreitol, Triton X-100 and lysozyme were from Boehringer (Lewes, E. Sussex, U.K.). Triethanolamine was from BDH (Glasgow, Scotland, U.K.). Glycerol was from Fisons (Loughborough, Leics., U.K.). Bradford reagent was from Bio-Rad (St. Albans, Herts., U.K.). DMSO was from Koch-Light (Haverhill, Suffolk, U.K.). Rolipram was a gift from Schering A. G. (Berlin, Germany).

Culture of U87 cells

U87 MG cells (ATCC reference number HTB14) were cultured at 37 °C in DMEM containing 1 mM glutamine, 10 % (v/v) foetal calf serum and 5000 i.u./ml penicillin and 5000 i.u./ml streptomycin.

Isolation of human PDE 4B cDNA species

PDE4B2

A 1.6 kb partial PDE4B cDNA was isolated from a human eosinophil cDNA library (kindly provided by Dr. D. Simmons, Institute of Molecular Medicine, Oxford, U.K.) by hybridization. Briefly, 10^6 colonies were screened with a 700 bp *Pvu*2–*Bgl*2 fragment from the catalytic conserved region of human PDE 4A. The probe was labelled with [^{32}P]dCTP (Amersham International) by random priming (Boehringer Mannheim) and filters were given a final wash in 0.2 × SSC/0.1 % SDS at 50 °C. A single positive clone was obtained, sequenced on both strands and shown to code for the entire catalytic domain and 3′ end of PDE4B2. The 5′ end of the human PDE4B2 sequence was then isolated by PCR by using published sequence information [20]. With the use of DNA prepared from the eosinophil cDNA library, a 0.67 kb fragment was amplified with primers P1 (5′-TTTTTAAGCTTAGCGTGCAAATAATGAAGG-3′) and P2 (5′-TTTTTAAGCTTACATGTAGGTTATAAATGTGTC-3′) and conditions of 94 °C for 1 min, 55 °C for 1 min and 72 °C for 1 min, for 30 cycles. A full-length PDE4B2 cDNA was constructed by joining the 5′ 0.67 kb fragment to the 1.6 kb partial cDNA by a strand-overlap PCR method. The final construct was inserted into the expression vector pEE7 to produce the plasmid pdeos20 (see Figure 1).

PDE4B1 and PDE4B3

Total RNA was prepared from U87 cells by using RNAzol and poly(A)$^+$ mRNA selected by affinity chromatography with oligo-(dT)-cellulose. First-strand cDNA was synthesized from 2 μg of poly(A)$^+$ mRNA with the 4B-specific primer (see Figure 1) P3 (5′-TTTTTGAATTCCACCAGTCTAATTCCTCCAGCGTTTCC-3′). Two rounds of 5′-RACE were then performed with the forward anchor primer (P4) supplied by the manufacturer and the following two nested reverse primers according to the 5′ Amplifinder® RACE protocol (Clontech, Palo Alto, CA, U.S.A.): P5, 5′-TTGAATTCGGAGGCTGACTAGCAGCTGGGGAC-3′; P6, 5′-GCTCTAGAGCTTGGAAGAGAAGAGTTTCTCGAC-3′.

The final PCR products were restricted with *Eco*R1 and *Xba*1, the sites in the anchor and the PDE4B primer respectively, and inserted into psp73 (Promega). The sequences of a number of independent clones were determined on both strands. Two different PDE4B 5′ ends were obtained: one corresponded to that reported previously for HSPDE4B1 [20,22], whereas the other diverged from this sequence towards the 5′ end and was designated HSPDE4B3 (see Figure 2). Further PCR amplifications were performed to reconstruct full-length cDNA species of these PDE4B variants. First, the 1.18 and 0.63 kb 5′-end fragments of PDE4B1 and PDE4B3 respectively were amplified from the specifically primed U87 first-strand cDNA by using the following variant specific 5′ primers in combination with a common 3′ primer (P9) (see Figure 1) and the conditions 95 °C for 1 min, 60 °C for 1 min and 72 °C for 2 min over 35 cycles: P7, 5′-TTGCGGAATTCATAATGAAGAAAAGCAGGAGTGTG-3′; P8, 5′-TTAGAATTCATGACAGCAAAAGATTCTTCAAAGG-3′; P9, 5′-GCTCTAGACTAATTCCTCCAGCGTTTCCATTGC-3′. The PCR products were restricted with *Eco*R1 and *Xba*1, inserted into psp73 and sequenced.

Secondly, the 5′ PDE4B1 and PDE4B3 fragments were joined by strand-overlap PCR to the PDE 4B sequence, which is common to all the variants obtained for PDE4B. The resulting full-length cDNA species were inserted into the pEE7 expression vector to produce the plasmids pdeos40 (PDE4B1) and pdeos41 (PDE4B3).

Reverse transcriptase–PCR (RT–PCR) analyses of human RNA

Poly(A)$^+$ mRNA from human heart and human brain was obtained from Clontech Laboratories. First-strand cDNA was synthesized from 150 ng of poly(A)$^+$ mRNA with a Pharmacia Biotech First Strand cDNA Synthesis Kit (Cat No 27-9261-01). Essentially, 150 ng of mRNA in diethyl pyrocarbonate-treated water, in a final volume of 20 μl, was denatured by heating to

65 °C for 10 min and then cooling immediately on ice. To this was added 11 μl of 'Bulk strand' cDNA mix, 1 μl of dithiothreitol (200 mM aqueous solution) and 1 μl of 'Not-1-d(T) 18' primer (0.2 μg/μl). The resultant solution was then mixed gently, incubated for 1 h at 37 °C and stored at −70 °C until use.

For HSPDE4B1 the sense primer used was GGAGAGGGAGAAGGTGTTGC and the anti-sense primer used was TGTGTCAGCTCCCGGTTCAGC. This was predicted to yield a fragment of 662 bp. Amplification conditions were 94 °C for 2 min followed by 35 cycles of 94 °C for 1 min, 55 °C for 2 min and 72 °C for 3 min. For HSPDE4B2 the sense primer sequence was AGCGGTGGTAGCGGTGACTC and the anti-sense primer was GCTGCGTGCAGGGTGTTGTG. This was predicted to amplify a fragment of 680 bp under conditions of one cycle at 95 °C for 1 min followed by 35 cycles at 63 °C for 2 min and 72 °C for 3 min. For HSPDE4B3 the sense primer was CTCCACGCAGTTCACCAAGGAAC and the anti-sense primer was TGTGTCAGCTCCCGGTTCAGC. This was predicted to yield a fragment of 598 bp under conditions of amplification of one cycle at 95 °C for 1 min followed by 35 cycles of 63 °C for 2 min and 72 °C for 3 min.

For each species, single bands of the expected sizes were isolated and the DNA was extracted with the Qiaex II Gel Extraction Kit (Qiagen). The isolated DNA was then ligated with the pCR2.1 TA cloning vector (Invitrogen) with blue/white screening. A total of six individual colonies for each species were isolated and sequenced in both directions with the *Taq* DyeDeoxy Terminator Cycle Sequencing Kit (Applied Biosystems).

Isolation of a novel rat PDE4B cDNA

A rat olfactory lobe cDNA library that had been cloned into the *Eco*RI sites of Lambda ZAP [43] was obtained from Stratagene (La Jolla, CA, U.S.A.) and screened as described in [44]. A probe corresponding to nt 1676–1877 of pRPDE6 (RNPDE4A5) [45] was used, with the final wash performed with 0.3 × SSC/0.3 % SDS at 65 °C. This probe corresponds to the N-terminal half of the UCR1 region of pRPDE6 [45] and reflects a region found to be common to all long-form PDE4 isoforms [3,9,20]. Sequencing was performed with an ABI PRISM sequencer (Perkin Elmer) in accordance with the manufacturer's instructions. Alignments were performed with the Intelligenetics suite of programs (Intelligenetics, Mountain View, CA, U.S.A.).

Generation of antisera to PDE4B

Two sets of antiserum were used in this study. Both of these exploit the fact that all of these PDE4B splice variants differed only at their extreme N-terminal ends, owing to 5′ domain swapping, but had identical C-terminal regions ([20,22], and this study). One antiserum used was that described previously by us [46] and was raised against a dodecapeptide that represents the extreme C-terminal region of these PDEs and, with one residue difference, is conserved between rodents and man. The second antiserum was generated against a GST fusion protein with procedures described elsewhere in detail by us for generating PDE4A-specific antiserum [37]. The GST fusion protein was constructed by introducing *Bam*H1 and *Eco*R1 restriction enzyme sites at positions 1547 bp and 1672 bp respectively of PDE4B2 and inserting the fragment obtained into the plasmid pGEX2T (Pharmacia Biotech, St. Albans, Herts., U.K.). This permitted the generation of a fusion protein, called GST-PDE4B45, which allowed in-frame expression of GST fused to a 45-residue C-terminal fragment found to be common to all PDE4B forms. None of these antisera showed cross-reactivity with recombinant human PDE4A, PDE4C or PDE4D forms expressed in COS cells (results not shown).

Quantification of PDE4B immunoreactive species with an ELISA method

Cell extract (0.4–50 μg) was incubated overnight at 4 °C in a final volume of 100 μl of bicarbonate buffer, pH 9.6 (Sigma C-3041) in 96-well plates. Plates were washed three times in Tris-buffered saline, pH 7.4, containing 0.05 % (v/v) Tween-20 (TBS/Tween-20), before being blocked in 1 % (w/v) powdered milk for 2 h at room temperature. After three washes in TBS/Tween-20, plates were incubated for 2 h at room temperature with primary antibody (1:1000 dilution) in TBS containing 0.1 % powdered milk. Plates were again washed in TBS/Tween-20 and incubated with secondary antibody conjugated with alkaline phosphatase (1:30000 dilution) in 0.1 % powdered milk for 1 h at room temperature. A further six washes in TBS/Tween-20 were followed by the addition of 100 μl of substrate (*p*-nitrophenyl phosphate) at 1 mg/ml in a buffer containing 0.1 M glycine, 1 mM $ZnCl_2$ and 1 mM $MgCl_2$, pH 10.4. After 30–60 min of incubation in the dark, A_{405} was read on a multiplate reader.

Transfection of COS-7 cells, and isolation and treatment of cytosol and pellet fractions

COS-7 cells were seeded at approx. one-third confluency on 10 cm diameter plates, 18 h before the transfection. Immediately before transfection the culture medium was replaced with 5 ml of DMEM supplemented with 10 % (v/v) Nuserum together with 0.1 mM chloroquine. This solution was prepared by diluting the DNA to 250 μl in TE buffer [10 mM Tris/HCl/0.1 mM EDTA (pH 7.6)] and adding 200 μl of a 10 mg/ml DEAE-dextran solution. The mixture was incubated at room temperature for 15 min before addition to the COS-7 cell culture. The cells were incubated for 3–4 h at 37 °C in an air/CO_2 (19:1) atmosphere before the medium was aspirated and the COS cell culture osmotically shocked for 2 min with 10 % (v/v) DMSO in PBS. The culture was then rinsed twice in PBS before DMEM containing 10 % (v/v) foetal calf serum was added; the cells were incubated at 37 °C in an air/CO_2 (19:1) atmosphere for 72 h.

Disruption of COS cells was done as described previously by us [31]. This was done in KHEM buffer [50 mM KCl/50 mM Hepes/KOH (pH 7.2)/10 mM EGTA/1.92 mM $MgCl_2$] containing 1 mM dithiothreitol and a mixture of protease inhibitors at final concentrations of 40 μg/ml PMSF, 156 μg/ml benzamidine, 1 μg/ml aprotinin, 1 μg/ml leupeptin, 1 μg/ml pepstatin A and 1 μg/ml antipain. Pellet fractions were also resuspended in this mixture. The high-speed (P2) pellet fraction was generated essentially as described previously by us [31,34,35]. This procedure routinely yielded a P1 pellet (1000 $\boldsymbol{g}_{av}$ for 10 min) and a P2 pellet (60 min at 100000 $\boldsymbol{g}_{av}$) as well as a high-speed supernatant (S). The homogenization procedure was complete in that no detectable latent lactate dehydrogenase activity was present in the P1 pellet, indicating an absence of cytosol proteins. Pellet fractions were treated with either the non-ionic detergent Triton X-100 (5 %, v/v), high [NaCl] (2 M) or both Triton X-100 and high [NaCl] added together, as described previously [30].

Relative activity determinations

This was done with a modification of the methodology described before by us [30,31,35]. To define K_m and V_{max}, data from PDE assays done over a range of cAMP substrate concentrations were analysed by computer-fitting to the hyperbolic form of the

Michaelis–Menten equation with an iterative least-squares procedure (Ultrafit; with Marquardt algorithm, robust fit, experimental errors supplied; Biosoft, Cambridge, U.K.). Relative V_{max} values were obtained by assessing the relative levels of each of these PDE4B isoforms immunologically. Briefly, increasing concentrations of protein (2–50 μg) from COS-7 cells transfected with the PDE4B isoforms were analysed with the ELISA technique described above. Quantitative data were obtained from absorbance measurements, which allowed plots of absorbance against mass of sample protein applied to be generated, to allow us to gauge the relative concentrations of particular PDE4B isoforms in different transfection experiments and between various subcellular fractions. For the V_{max} determinations, amounts of protein from transfected COS-7 cells that would provide equal amounts of these various PDE4B species were taken. They were then assayed for PDE activity with V_{max} determined from data obtained from full Michaelis–Menten plots with the fitting algorithms described above.

PDE assay

Cyclic nucleotide PDE activity was assayed by a modification of the two-step procedure of Thompson and Appleman [47] and Rutten et al. [48], as described previously by Marchmont and Houslay [16]. All assays were conducted at 30 °C and in all experiments a freshly prepared slurry of Dowex/water/ethanol (1:1:1, w/v/v) was used for determination of activities. Initial rates were taken from linear time courses of activity. For the determination of kinetic parameters, the PDE assays were conducted with 10–15 different cAMP concentrations over a range from 0.1 to 100 μM. As indicated below, the COS7 cell transfection procedure used in this study led to very high levels of novel PDE4 activity being produced, such that this comprised more than 94% of the total COS cell PDE activity. Mock transfections, with vector only, as indicated in previous studies [30,31,34,35], did not alter the endogenous COS cell PDE activity. As a routine, however, we subtracted the residual endogenous COS cell PDE activities done in parallel experiments from those activities found in the PDE4B-transfected cells. Protein was routinely measured by the method of Bradford [49], with BSA as a standard.

SDS/PAGE and Western blotting

Polyacrylamide gels (8%, w/v) were used and the samples boiled for 3 min after being resuspended in Laemmli [50] buffer. Gels were run at 8 mA per gel overnight or 50 mA per gel for 4–5 h, with cooling. For detection of transfected PDE by Western Blotting, 2–50 μg protein samples were separated by SDS/PAGE and then transferred to nitrocellulose before being immunoblotted with human PDE4B antisera. Labelled bands were identified by using peroxidase-linked anti-(rabbit IgG); either Amersham enhanced chemiluminescence Western blotting was used as a detection protocol or ^{125}I-labelled anti-rabbit antiserum was used for detection and quantification.

RESULTS

Molecular cloning

Two splice junctions have been identified that lead to distinct isoform products from the PDE4A and PDE4D genes [3,9,20,51]. Alternative mRNA splicing at the first of these yields long-form PDE4 products that contain the complete upstream conserved regions (UCRs) 1 and 2 [3,20]. These UCRs are found towards the N-terminus of PDE4 isoforms and provide unique signatures of the cAMP-specific PDE4 multi-gene family, which even encompass the cognate *Drosophila melanogaster dunc* PDE [9]. A second site of mRNA splicing is also seen for these mammalian PDE4 genes. This yields 'short' isoforms that lack UCR1. Comparing the reported human PDE4B genes it is evident that HSPDE4B2 [3,20] reflects a short-form product lacking UCR1, whereas HSPDE4B1 [3,20,22] is a long-form product that possesses both UCR1 and UCR2. To search for novel PDE4B splice variants we used the 5′-RACE method with two nested reverse primers that were located upstream of the divergence point occurring between the previously characterized long (PDE4B1) and short (PDE4B2) forms of PDE4B [3,20,22]. This was performed on poly(A)$^+$ RNA extracted from the human glioblastoma U87 cell line (Figure 1). By doing this we isolated a novel 5′ end sequence that corresponded to a 'long'-form product of the human PDE4B gene as it contained both UCR1 and UCR2. The identification of such a second 'long' form of PDE4B thus provides definition for the PDE4B gene of the existence of a second splice site that is cognate to that seen in *D. melanogaster* and to those found in the PDE4A and PDE4D genes, which yield distinct long-form splice variants [6,30,45]. The ORF encompassing this novel 5′ sequence encodes a protein that we call PDE4B3 (Figure 2). This is 721 residues in length, compared with the 736 residues of PDE4B1 [22] and 564 residues of PDE4B2 [20]. The parts of the N-terminal alternatively spliced region that is unique to each of these three species are 94, 39 and 79 residues for PDE4B1, PDE4B2 and PDE4B3 respectively.

We and others have previously described the isolation of cDNA clones derived from two different mRNA transcripts from the rat PDE4B gene [19,41,45,52]. The first of these to be isolated, called pDPD, encodes the RNPDE4B1 isoform [41]. Although pDPD encodes a functional, rolipram-inhibited cAMP-specific PDE, its ORF of 562 residues is not complete but extends beyond the 5′ end of the clone. Full-length cDNA clones (pRPDE18 and ratPDE2) encoding a second rat PDE4B isoform, RNPDE4B2, have been isolated by us and by others, and encode a protein of 564 residues [45,52]. To isolate cDNA clones encoding additional splice variants from the PDE4B locus, a rat olfactory lobe cDNA library was screened with a probe that corresponded to UCR1 from the rat PDE4A5 cDNA, pRPDE6 [45]. Such a conserved region characterizes all long PDE4 isoforms; a probe that reflects this region can therefore be expected to be of use in trying to identify novel long-form PDE4 splice variants, irrespective of which of the four PDE4 gene families they belong to. Among the cDNA species isolated in this screening was pRPDE74, which contained an ORF encoding 721 residues. The sequence of the putative protein encoded by pRPDE74 was highly similar (Figure 1) to that of the novel human PDE4B3 isoform that we have identified in this study, with 96% amino acid identity. For this reason we refer to the protein encoded by pRPDE74 as RNPDE4B3. It is therefore reassuring that homologous human and rat species have been identified by using these two different cloning procedures, thus confirming the identity of the novel N-terminal alternatively spliced sequence found in these cognate PDE4B3 species.

Interestingly, the amino acid sequence of the pDPD ORF [41] is entirely included in that of pRPDE74 (i.e. the C-terminal 562 residues of the pRPDE74 protein are identical with all of the sequence encoded by the truncated ORF of pDPD). Therefore it is possible that pDPD is in fact a partial clone for the novel rat RNPDE4B3 isoform the we have identified in this study. Certainly our results showing an additional splice variant for the *PDE4B* genes indicates that the genomic structure of the rat *PDE4B* gene is more complex than has previously been reported [53].

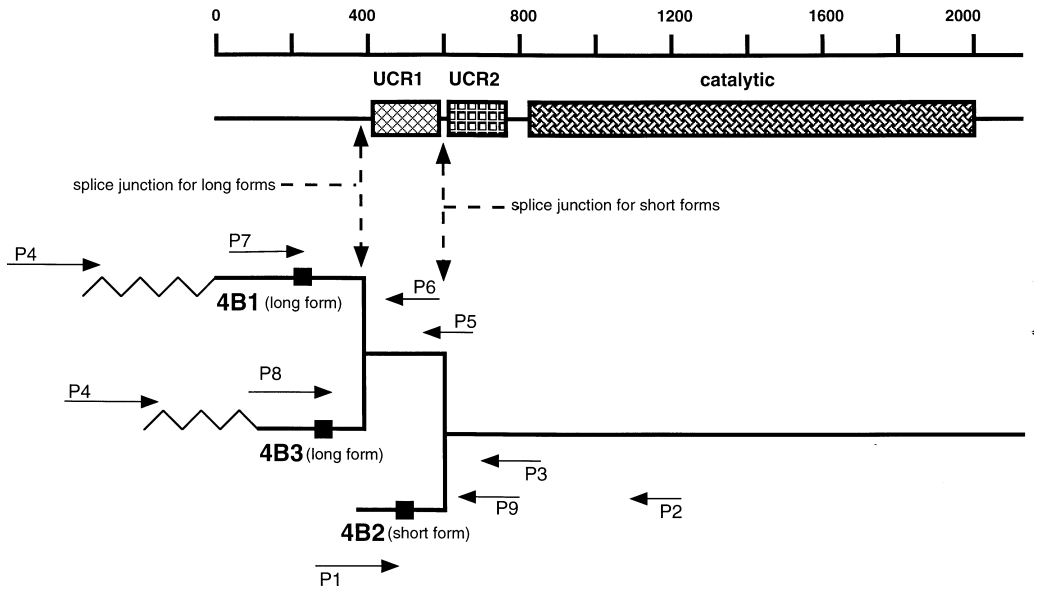

Figure 1 PCR primers used in the generation of PDE4B isoforms

A 1.6 kb partial PDE4B cDNA was isolated from a human eosinophil cDNA library and shown to code for the entire catalytic domain and 3′ end of PDE4B. To construct PDE4B2, the 5′ end of the human PDE4B2 sequence was then isolated by PCR with the use of published sequence information [20]. By using DNA prepared from the eosinophil cDNA library, a 0.67 kb fragment was amplified with the primers P1 and P2. A full-length PDE4B2 cDNA was constructed by joining the 5′ 0.67 kb fragment to the 1.6 kb partial cDNA by the strand-overlap PCR method. The final construct was inserted into the expression vector pEE7 to produce the plasmid pdeos20 for PDE4B2. Generation of PDE4B1 and the novel PDE4B3 involved first strand cDNA being synthesized from 2 μg of poly(A)$^+$ mRNA with the 4B-specific primer P3. Two rounds of 5′-RACE were then performed with the forward anchor primer (P4) and the two nested reverse primers P5 and P6. The final PCR products were restricted with *Eco*R1 and *Xba*1, the sites in the anchor and the PDE4B primer respectively, and inserted into psp73. Further PCR amplifications were performed to reconstruct full-length cDNA species of the PDE4B1 and PDE4B3 variants. The 1.18 and 0.63 kb 5′ end fragments of PDE4B1 and PDE4B3 respectively were amplified from the specifically primed U87 first-strand cDNA by using the P7 and P8 variant-specific 5′ primers in combination with a common 3′ primer P9. The 5′ PDE4B1 and PDE4B3 fragments were joined by strand-overlap PCR to the PDE 4B sequence that is common to all the variants obtained for PDE4B. The resulting full-length cDNA species were inserted into the pEE7 expression vector to produce the plasmids pdeos40 (PDE4B1) and pdeos41 (PDE4B3).

Immunological detection of PDE4B isoforms expressed transiently in COS7 cells

Immunoblotting of transfected COS cells allowed us to detect (Figure 3) a novel immunoreactive species in COS7 cells transfected with each of the plasmids containing the various PDE4B cDNA species. Single immunoreactive species were found for both HSPDE4B1, at 104 ± 3 kDa, and HSPDE4B3, at 103 ± 2 kDa (means $\pm$ S.D., $n = 3$). However, for HSPDE4B2, whereas a major band at 78 ± 4 kDa was found in the cytosol, a doublet containing both a species of this size and a larger one of 85 ± 3 kDa was found in the particulate fractions (means $\pm$ S.D., $n = 3$). The sizes of these forms, which can be predicted from their primary sequences, were 84, 64 and 82 kDa for PDE4B1, PDE4B2 and PDE4B3 respectively.

Such immunoreactive species were found distributed between the cytosol (high-speed supernatant), the low-speed pellet (P1) and the high-speed pellet (P2) fractions (Figure 3). The distribution between these three fractions is shown in Table 1. The pellet fractions were subjected to four different procedures to determine the susceptibility of immunoreactive PDE4B forms to release. These involved incubation with either buffer (KHEM) alone or in the presence of either the non-ionic detergent Triton X-100 (5%), high [NaCl] (2 M) or both Triton X-100 and high [NaCl] together. After this the samples were subjected to high-speed centrifugation to isolate the treated pellet and high-speed supernatant fractions. These were then analysed by SDS/PAGE to determine whether such treatments had caused the release of the immunoreactive PDE4B species (Table 1). In no instance, with any of the isoforms, did simply washing the pellet fractions with DMEM cause the release of immunoreactive material (less than 5%). Treatment of the P2 pellets with Triton X-100 seemed to elicit the release of approx. 50% of the immunoreactive PDE4B1 and PDE4B2 species but had no effect on the release of PDE4B3 (Table 1). Similar results were obtained when Triton X-100 and NaCl were used in concert. However, high [NaCl] solutions alone did not cause the release of any of these species, indicating that association was not governed primarily by ionic interactions. In contrast with this, whereas immunoreactive PDE4B1 and PDE4B2 forms were not released from the P1 pellet fraction by washing with buffer alone, they were totally released by high [NaCl]. This suggests that these isoforms associated with species in the P1 and P2 pellet fractions in very different ways. Evidently in the P1 fraction they associated with detergent-insoluble species through ionic interactions. Although PDE4B3 was also released from the P1 fraction by high [NaCl], in contrast with the other two PDE4B forms it was also released by Triton X-100. It therefore seems that there are distinct differences in the way in which these various PDE4B isoforms interact with species in the P1 and P2 pellet fractions.

K_m (cAMP) and relative V_{max} values of PDE4B splice variants expressed in transfected COS7 cells

The cAMP-PDE activity of all of these transfected enzymes was not stimulated by the addition of Ca^{2+}/calmodulin, which can be expected to activate PDE1, nor was it altered by the low cGMP concentrations (10 μM) expected either to inhibit PDE3 or to activate PDE2 [2,5,8,51]. The activity of the novel PDE4B3, as

(a)

```
hspde4b3    1                mtakdsskeltasepevciktfkeqmhlelelprlpgnrptspkis

hspde4b1    1 mkksrsvmtvmaddnvkdyfecslsksyssssntlgidlwrgrrccsgnlqlpplsqrqse

hspde4b3   47 prssprnspcffrkllvnksirqrrrftvahtcFDVENGPSPGRSPLDPQASSSAGLVLHA
                                             ||||||||||||||||||||||||||||||
hspde4b1   62 rartpegdgisrpttlplttlpsiaittvsqecFDVENGPSPGRSPLDPQASSSAGLVLHA

hspde4b2    1                                                  mkehggtfsst

hspde4b3  108 TFPGHSQRRESFLYRSDSDYDLSPKAMSRNSSLPSEQHGDDLIVTPFAQVLASLRSVRNNF
              ||||||||||||||||||||||||||||||||||||||||||||||||||||||||||||||
hspde4b1  123 TFPGHSQRRESFLYRSDSDYDLSPKAMSRNSSLPSEQHGDDLIVTPFAQVLASLRSVRNNF

hspde4b2   12 gisggsgdsamdslqplqpnymqvclfaEESYQKLAMETLEELDWCLDQLETIQTYRSVSE------
                                            ||||||||||||||||||||||||||||||||
hspde4b3  169 TILTNLHGTSNKRSPAASQPPVSRVNPQEESYQKLAMETLEELDWCLDQLETIQTYRSVSE------
              ||||||||||||||||||||||||||||||||||||||||||||||||||||||||||||||
hspde4b1  184 TILTNLHGTSNKRSPAASQPPVSRVNPQEESYQKLAMETLEELDWCLDQLETIQTYRSVSE------
```

(b)

```
hspde4b3    1 MTAKdSSKELtASEpEVCIKTFKEQMhLELELPrLPGNRPTSPKISPRSSPRNSPCFFRKL
              |||| ||||| ||| |||||||||||| |||||| ||||||||||||||||||||||||||
rnpde4b3    1 MTAKnSSKELpASEsEVCIKTFKEQMrLELELPkLPGNRPTSPKISPRSSPRNSPCFFRKL

consensus       MTAK-SSKEL-ASE-EVCIKTFKEQM-LELELP-LPGNRPTSPKISPRSSPRNSPCFFRKL

hspde4b3   62 LVNKSIRQRRRFTVAHTCFDVENGPSPGRSPLDPQASSSaGLVLHAtFPGHSQRRESFLYR
              ||||||||||||||||||||||||||||||||||||||| |||||| ||||||||||||||
rnpde4b3   62 LVNKSIRQRRRFTVAHTCFDVENGPSPGRSPLDPQASSSsGLVLHAaFPGHSQRRESFLYR

consensus       LVNKSIRQRRRFTVAHTCFDVENGPSPGRSPLDPQASSS-GLVLHA-FPGHSQRRESFLYR

hspde4b3  123 SDSDYDLSPKAMSRNSSLPSEQHGDDLIVTPFAQVLASLRsVRNNFTiLTNLHGtsNKRSP
              ||||||||||||||||||||||||||||||||||||||| |||||| ||||||  |||||
rnpde4b3  123 SDSDYDLSPKAMSRNSSLPSEQHGDDLIVTPFAQVLASLRiVRNNFTlLTNLHGapNKRSP

consensus       SDSDYDLSPKAMSRNSSLPSEQHGDDLIVTPFAQVLASLR-VRNNFT-LTNLHG--NKRSP

hspde4b3  184 AASQpPVsRVnpQEESYQKLAMETLEELDWCLDQLETIQTYRSVSEMASNKFKRMLNRELT
              |||| || ||  |||||||||||||||||||||||||||||||||||||||||||||||||||
rnpde4b3  184 AASQaPVtRVslQEESYQKLAMETLEELDWCLDQLETIQTYRSVSEMASNKFKRMLNRELT

consensus       AASQ-PV-RV--QEESYQKLAMETLEELDWCLDQLETIQTYRSVSEMASNKFKRMLNRELT

hspde4b3  245 HLSEMSRSGNQVSEYISNTFLDKQNDVEIPSPTQKDREKKKKQQLMTQISGVKKLMHSSSL
              ||||||||||||||||||||||||||||||||||||||||||||||||||||||||||||||
rnpde4b3  245 HLSEMSRSGNQVSEYISNTFLDKQNDVEIPSPTQKDREKKKKQQLMTQISGVKKLMHSSSL

consensus       HLSEMSRSGNQVSEYISNTFLDKQNDVEIPSPTQKDREKKKKQQLMTQISGVKKLMHSSSL

hspde4b3  306 NNTSISRFGVNTENEDHLAKELEDLNKWGLNIFNVAGYSHNRPLTCIMYAIFQERDLLKTF
              ||||||||||||||||||||||||||||||||||||||||||||||||||||||||||||||
rnpde4b3  306 NNTSISRFGVNTENEDHLAKELEDLNKWGLNIFNVAGYSHNRPLTCIMYAIFQERDLLKTF

consensus       NNTSISRFGVNTENEDHLAKELEDLNKWGLNIFNVAGYSHNRPLTCIMYAIFQERDLLKTF

hspde4b3  367 rISSDTFiTYMMTLEDHYHSDVAYHNSLHAADVAQSTHVLLSTPALDAVFTDLEILAAIFA
               |||||| ||||||||||||||||||||||||||||||||||||||||||||||||||||||
rnpde4b3  367 kISSDTFvTYMMTLEDHYHSDVAYHNSLHAADVAQSTHVLLSTPALDAVFTDLEILAAIFA

consensus       -ISSDTF-TYMMTLEDHYHSDVAYHNSLHAADVAQSTHVLLSTPALDAVFTDLEILAAIFA

hspde4b3  428 AAIHDVDHPGVSNQFLINTNSELALMYNDESVLENHHLAVGFKLLQEEHCDIFmNLTKKQR
              ||||||||||||||||||||||||||||||||||||||||||||||||||| |||||||
rnpde4b3  428 AAIHDVDHPGVSNQFLINTNSELALMYNDESVLENHHLAVGFKLLQEEHCDIFqNLTKKQR

consensus       AAIHDVDHPGVSNQFLINTNSELALMYNDESVLENHHLAVGFKLLQEEHCDIF-NLTKKQR

hspde4b3  489 QTLRKMVIDMVLATDMSKHMSLLADLKTMVETKKVTSSGVLLLDNYTDRIQVLRNMVHCAD
              ||||||||||||||||||||||||||||||||||||||||||||||||||||||||||||||
rnpde4b3  489 QTLRKMVIDMVLATDMSKHMSLLADLKTMVETKKVTSSGVLLLDNYTDRIQVLRNMVHCAD

consensus       QTLRKMVIDMVLATDMSKHMSLLADLKTMVETKKVTSSGVLLLDNYTDRIQVLRNMVHCAD

hspde4b3  550 LSNPTKSLELYRQWTDRIMEEFFQQGDKERERGMEISPMCDKHTASVEKSQVGFIDYIVHP
              ||||||||||||||||||||||||||||||||||||||||||||||||||||||||||||||
rnpde4b3  550 LSNPTKSLELYRQWTDRIMEEFFQQGDKERERGMEISPMCDKHTASVEKSQVGFIDYIVHP

consensus       LSNPTKSLELYRQWTDRIMEEFFQQGDKERERGMEISPMCDKHTASVEKSQVGFIDYIVHP

hspde4b3  611 LWETWADLVQPDAQDILDTLEDNRNWYQSMIPQSPSPPLDEqnRDCQGLMEKFQFELTLdE
              |||||||||||||||||||||||||||||||||||||||  ||||||||||||||| |
rnpde4b3  611 LWETWADLVQPDAQDILDTLEDNRNWYQSMIPQSPSPPLDErsRDCQGLMEKFQFELTLeE

consensus       LWETWADLVQPDAQDILDTLEDNRNWYQSMIPQSPSPPLDE--RDCQGLMEKFQFELTL-E

hspde4b3  672 EDSEGPEKEGEGhsYFSSTKTLCVIDPENRDSLgETDIDIATEDKSpvDT
              |||||||||||  ||||||||||||||||||| |||||||||||  ||
rnpde4b3  672 EDSEGPEKEGEGpnYFSSTKTLCVIDPENRDSLeETDIDIATEDKSliDT

consensus       EDSEGPEKEGEG--YFSSTKTLCVIDPENRDSL-ETDIDIATEDKS--DT
```

Figure 2 Sequence of the novel PDE4B3 splice variants

(**a**) Comparison of amino acid sequences of the unique N-terminal regions of the three human PDE4B isoforms. Amino acid sequences continue as an identical sequence for all three isoforms after the sequence 'VSE' and are given in full in (**b**) for human PDE4B3 together with a comparison of the predicted amino acid sequences of the novel human HSPDE4B3 and the novel RNPDE4B3, the proposed cognate rat form encoded by pRPDE74, together with the consensus sequence.

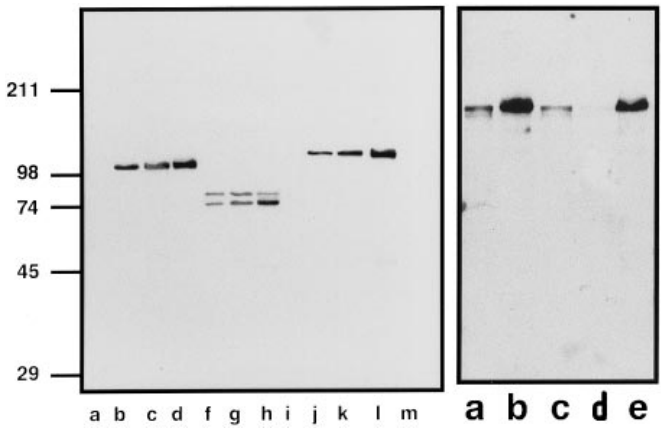

Figure 3 Immunodetection of human PDE4B3

In the experiment shown in the left-hand panel, COS7 cells were transiently transfected with plasmids encoding the three HSPDE4B isoforms before cell disruption, subcellular fractionation and analysis by SDS/PAGE, and subsequent immunoblotting. Shown are data for HSPDE4B1 (tracks j, k and l), HSPDE4B2 (tracks f, g and h) and HSPDE4B3 (tracks b, c and d) isoforms with an analysis of high-speed supernatant (tracks d, h and l) as well as particulate P1 (tracks b, f and j) and P2 (tracks c, g and k) pellet fractions generated as described in the Materials and methods section. Detection of immunoreactive species was done with PDE4B-specific antiserum. The results are typical of experiments done at least three times. Results are also shown for untransfected cells (track a) and for cells transfected with control vector (track m). The positions of molecular-mass markers are shown at the left in kDa. Right-hand panel: immunoblot for a homogenate of U87 cells (tracks a and c), HSPDE4B1-transfected COS cells (track b), non-transfected COS cells (track d) and HSPDE4B3-transfected COS cells (track e).

well as that of the 4B1 and 4B2 forms, was, however, inhibited (more than 96 %) by the addition of the PDE4-selective inhibitor rolipram (10 μM). This is consistent with these enzymes' being PDE4 isoforms. The K_m values for cAMP substrate utilization for all these isoforms, irrespective of their subcellular localization, were similar and in the range 1.4–2.6 μM (Table 2). These values are somewhat lower than those reported previously for 4B1 (7.2–8.5 μM) and 4B2 (4.3 μM), but those studies were made on species expressed in either *Saccharomyces cerevisiae* or *Echerichia coli* and, in one instance, analyses were made on severely N-terminally truncated species [20,22]. The values we report for the full-length PDE4B species expressed in COS7 cells, however, are similar to those that we have found for various PDE4D splice variants (0.7–1.3 μM) expressed in COS7 cells but slightly lower than those that we have reported for various PDE4A splice variants (1.9–5.4 μM) expressed in COS cells [30,31,34,35,37].

Immunoblotting analyses made on COS cells transfected so as to express the three different isoforms allowed us to determine the relative concentration of each isoform and also to calculate the relative amounts of each immunoreactive species in both the cytosol and particulate fractions. However, here we have also developed an ELISA method that allows a rapid and simple method of quantification. Determination of the relative activities of these PDE4B forms cannot be done simply by comparing PDE activities in transfected cells, as activities are influenced by any differences in the levels of transfection. To obviate this we have used an immunological detection procedure to determine the relative expression levels of each of these isoforms in different transfection experiments. This allowed us to determine relative V_{max} values for the various PDE4B isoforms that take account of differences in expression levels. The activities of the cytosol-expressed components of these various PDE4B isoforms were determined relative to that of the long-form PDE4B1, which was set arbitrarily at unity. This allowed us to show that, whereas the V_{max} of the other long form, PDE4B3, was slightly higher than

Table 1 Distribution of PDE4B isoforms in transfected COS7 cells

COS7 cells were transiently transfected with plasmids containing the cDNA species for the indicated PDE4B isoforms. Cells were then harvested and disrupted as described in the Materials and methods section so as to produce a high-speed supernatant fraction together with low-speed pellet (P1) and high-speed pellet (P2) fractions. The percentage distribution of immunoreactive PDE4B species between these various fractions is shown. Results are given as means ± S.D. for $n = 3$ separate experiments with different transfected cell preparations. The various pellet/particulate fractions were then treated, as described in the Materials and methods section, with either the non-ionic detergent Triton X-100 (5%) alone, high (2 M) [NaCl] or both detergent and high [NaCl] together before centrifugation to determine the percentage release of immunoreactive PDE4B species. At the same time incubations were done with DMEM buffer alone; in this case the release of immunoreactive species was less than 5% for all of the PDE4B forms from either the P1 or the P2 pellet. Results are given as a range for $n = 3$ separate experiments with different transfected cell preparations except when either essentially all or none of the immunoreactive material was released.

	Distribution (%)			P1 release (%)			P2 release (%)		
	Supernatant	P1	P2	Triton X-100	High [NaCl]	Triton + NaCl	Triton X-100	High [NaCl]	Triton + NaCl
4B1 (long)	71 ± 3	17 ± 2	11 ± 2	< 3	> 98	> 98	58/72	< 5	56/67
4B2 (short)	61 ± 3	26 ± 2	12 ± 2	48/62	> 98	> 98	55/76	< 8	47/63
4B3 (long)	58 ± 5	23 ± 2	17 ± 4	76/88	> 98	> 98	< 4	< 3	< 2

Table 2 Kinetic constants for PDE4B isoforms

Analyses were performed as described in the Materials and methods section. Results are means ± S.D. for $n = 3$ experiments, with the use of different cell transfections with plasmids encoding the indicated PDE4B isoforms. V_{max} values for cytosol forms are given relative to that observed for PDE4B1, which is set at unity for comparison. The relative amounts of each of the PDE4B isoforms in experiments were determined immunologically (see the Materials and methods section). This allowed for the determination of relative V_{max} values, as corrections could be made for the different levels of expression of the different PDE4B isoforms in the various transfections and between the various subcellular fractions. Thus the relative V_{max} values represent true differences in the catalytic activity of the PDE4B isoforms. To determine whether association with the pellet fractions altered the V_{max} values for the various PDE4B isoforms, a ratio of the relative activity for the particulate/cytosol activity is given for the P1 and P2 components relating to each of the isoforms. For rolipram inhibition the IC_{50} values and Hill coefficients are shown; results are means ± SD for $n = 3$ experiments with the use of different cell transfections with plasmids encoding the indicated PDE4B isoforms.

	K_m (cAMP) (μM)			V_{max} relative to PDE4B1	V_{max} relative to appropriate cytosol form		IC_{50} (rolipram) (μM)			Hill coefficient (rolipram)		
	Cytosol	P2	P1	Cytosol	P2	P1	Cytosol	P2	P1	Cytosol	P2	P1
PDE4B1	2.0 ± 0.7	1.4 ± 0.1	1.7 ± 0.2	(1.00)	0.33 ± 0.16	0.40 ± 0.11	0.08 ± 0.03	0.05 ± 0.01	0.10 ± 0.02	0.63 ± 0.01	0.61 ± 0.05	0.52 ± 0.05
PDE4B2	2.6 ± 0.7	2.2 ± 0.8	1.8 ± 0.4	3.8 ± 0.8	0.38 ± 0.14	0.44 ± 0.16	0.02 ± 0.01	0.21 ± 0.03	0.18 ± 0.04	0.58 ± 0.07	0.67 ± 0.05	0.50 ± 0.07
PDE4B3	1.5 ± 0.5	1.4 ± 0.1	1.9 ± 0.3	1.6 ± 0.2	0.92 ± 0.01	1.1 ± 0.1	0.05 ± 0.01	0.10 ± 0.03	0.14 ± 0.03	0.61 ± 0.0	0.69 ± 0.15	0.64 ± 0.06

that of PDE4B1 (Table 2), the relative V_{max} of the short form, PDE4B2, was considerably (approx. 4-fold) higher than that of PDE4B1 (Table 2).

We also wished to assess whether the association of these various isoforms with particulate components altered their intrinsic catalytic activity. In order to do this we determined the V_{max} of the particulate component of each isoform relative to the activity of the cytosolic component of each corresponding isoform. This showed that the particulate components, found in both the P1 and P2 fractions, of both the PDE4B1 and PDE4B2 isoforms had a maximal catalytic activity that was rather lower, at approx. 40% of that of the cytosol component of the corresponding PDE4B isoform (Table 2). In marked contrast with this, the relative V_{max} of particulate PDE4B3, found in both the P1 and P2 fractions, seemed to be similar to that of the cytosolic component. It is of interest that, in this regard, whereas both the PDE4B1 and PDE4B2 isoforms seemed to associate similarly with the particulate fractions, PDE4B3 seemed to interact in a distinct fashion.

Inhibition by rolipram of PDE4B splice variants expressed in COS7 cells

Dose–effect analyses for all isoforms with rolipram as an inhibitor showed similar shallow inhibition curves for all forms, whether in the cytosol or in the particulate-associated state (results not shown). This, however, is evident from observation that the Hill coefficients for such plots were less than unity (Table 2), implying non-Michaelis–Menten kinetics of inhibition. Indeed, abnormal kinetics of rolipram inhibition of PDE4B2, expressed in *S. cerevisiae*, has been noted [22]. Nevertheless dose–effect plots for the various PDE4B forms were clearly not identical. Thus a rank order of inhibition was defined as B2 B3 B1 for the cytosolic forms and B1 B3 B2 for the particulate forms, with IC_{50} values varying from 0.02 to 0.2 μM (Table 2). The PDE4B1 found in both cytosolic and particulate fractions showed similar sensitivities to inhibition by rolipram (Table 2). In marked contrast, the short form, PDE4B2, showed a approx. 10-fold difference in IC_{50} values for rolipram inhibition of the cytosol and particulate components of this isoform, and the novel PDE4B3 form showed a rather smaller, 2–3-fold difference (Table 2). Thus the short form, PDE4B2, had the highest affinity for inhibition by rolipram when it was in its cytosol-located state but the lowest when in its particulate-associated state.

RT–PCR analyses made on U87 cells and human brain and heart RNA

Primers specific for each of the long PDE4B forms were designed and used in RT–PCR analyses to detect the presence of transcripts in RNA prepared from U87 cells as well as human brain and heart RNA preparations. These were able to amplify fragments of the predicted size from only the appropriate PDE4B-expressing plasmids. Such primers permitted the amplification of fragments

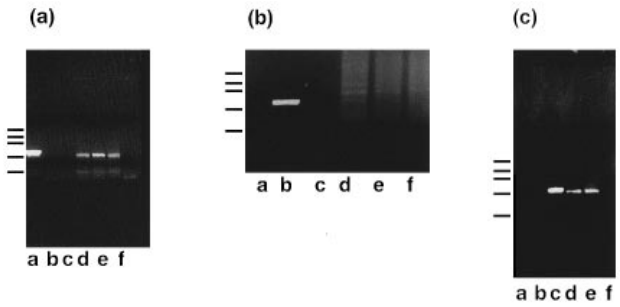

Figure 4 RT–PCR analyses of human brain and heart RNA

Primers specific for each of the HSPDE4B forms were used for RT–PCR analyses of COS cells transfected with plasmids encoding HSPDE4B1 (track a), HSPDE4B2 (track b) and HSPDE4B3 (track c) as well as RNA prepared from U87 cells (track d), human heart (track e) and human brain (track f). Primers specific for HSPDE4B1 were used in (**a**), for HSPDE4B2 in (**b**) and HSPDE4B3 in (**c**). The size markers indicated were 1353, 1078, 872, 603 and 301 bp. These results are typical of experiments done at least three times.

of the appropriate size for PDE4B1 from all these RNA sources but we were only able to amplify appropriate fragments for PDE4B3 from heart and U87 cells. The identities of these fragments were subsequently confirmed by sequencing. Thus heart and not brain seemed to exhibit transcripts for the novel PDE4B long form (Figure 4). Immunoblotting of U87 cells (Figure 3) showed an immunoreactive species that migrated at the position expected for the similarly sized PDE4B1 and PDE4B3 species, which is consistent with our detection (Figure 3) of transcripts for both of these long forms in these cells. However, no immunoreactive species indicative of the expression of PDE4B2 was observed (Figure 3), consistent with our inability to observe transcripts for this short form by RT–PCR analysis (results not shown).

DISCUSSION

We describe here the molecular cloning of a novel human splice variant, HSPDE4B3, together with that of its purported rat homologue RNPDE4B3, encoded by the plasmid pRPDE74. The identification of a second long–form PDE4B product indicates that alternative mRNA splicing of the PDE4B gene occurs at a cognate position to that seen providing the long forms of the PDE4A and PDE4D genes and at which alternative mRNA splicing is seen in *D. melanogaster* [3,51,54]. The structures of the cDNA species encoding these three human PDE4B isoforms are consistent with alternative splicing of their corresponding mRNA species, in which different 5′ exons are alternatively spliced to a 'core' region of the mRNA. For the long forms, HSPDE4B1 and HSPDE4B3, this 'core' region encompasses the UCR1 and the UCR2 regions as well as the catalytic domain of the protein. In contrast, HSPDE4B2 does not contain UCR1. So far the analysis of genomic clones for PDE4B has been limited to studies done on rodent genes [53] at a time when the long forms of PDE4B were unknown. Further analysis of genomic clones derived from either rodent or human PDE4B genes will be needed to confirm the hypothesis of alternative mRNA splicing yielding the so-called long forms. Nevertheless such a model is consistent with the proposed structure of the gene for the *Drosophila dunc* PDE [54].

The novel long isoform in human, PDE4B3, is very similar in size to that of the other known long-form product of the PDE4B gene, namely PDE4B1 [20,22], when they are detected immunologically in transfected COS7 cells. In situations where both of these isoforms are expressed together natively, such similarity in size will, however, make it very difficult indeed to discriminate between these two isoforms with immunoblotting procedures with antisera raised against common epitopes. Nevertheless the ability to design primers specific for each of these isoforms will allow RT–PCR analyses to provide a rapid and simple method of ascertaining whether transcripts for both such forms are present in RNA preparations. Indeed, the effectiveness of a similar strategy has been demonstrated for human PDE4D isoforms, where the HSPDE4D1 and HSPDE4D2 isoforms are very similar in size [55]. We show here that human U87 cells exhibit a 103 ± 2 kDa immunoreactive PDE4B species (Figure 3, left-hand panel). This, presumably, reflects the expression of both HSPDE4B1 and HSPDE4B3 because transcripts for both these two long isoforms can be detected by RT–PCR analyses (Figure 4).

It is intriguing that all three human PDE4B isoforms analysed here seem to reside in both cytosol and particulate compartments of transfected COS7 cells. This contrasts with PDE4A isoforms, which show isoform-specific distribution patterns, with particular isoforms being either exclusively particulate [31,36] or distributed between both particulate and cytosol fractions [30,31,37], and also with PDE4D isoforms expressed transiently in COS7 cells, where the short isoforms seem to be located entirely in the cytosol, whereas the long forms are differentially distributed between differently distributed between the cytosol and particulate fractions [56]. However, the various PDE4B isoforms show distinct patterns of release not only from each other but also between the low-speed (P1) and high-speed (P2) pellet fractions. Thus, although we were unable to solubilize the P2 pellet-associated form of PDE4B3 by using either the non-ionic detergent Triton X-100 or by using high [NaCl], detergent treatment was able to initiate the release of the P2 pellet-associated forms of both PDE4B1 and PDE4B2. This suggests either that these components might be binding to a membrane component through hydrophobic interactions or that they might be associating with an integral membrane protein that is solubilized by this detergent treatment. The inability to release PDE4B3 with any of these procedures is reminiscent of the association of the PDE4A forms PDE46 [37], RPDE6 [31] and RPDE39 [30]. This might reflect binding of these various PDE4 isoforms with cytoskeletal components associated with the P2 pellet fraction. Association of the various PDE4B isoforms with the P1 particulate fraction seemed to occur differently with that seen in the P2 fraction. For example, we were unable to solubilize PDE4B3 from the P2 fraction, whereas treatment of the P1 fraction with either Triton X-100 or high [NaCl] served to release this isoform. Furthermore, unlike the P2 pellet-associated components of PDE4B1 and PDE4B2, the P1-pellet components of these isoforms were resistant to release by Triton X-100 but were readily solubilized by high [NaCl]. Thus the P1 pellet populations of PDE4B1 and PDE4B2 seem to associate through ionic interactions with a detergent-insoluble species, which might represent a cytoskeletal component. That the PDE4B3 component found in the P1 pellet is released by either detergent or high [NaCl] might imply association through ionic interactions with a membrane component. In any event, it seems that distinct means are available to effect the intracellular targeting of these isoforms and that more than one anchor site for each of these enzymes might occur in COS cells. That these isoforms differ solely at their N-terminal splice regions is consistent with the notion [34] that a key role of such domains is to effect the intracellular targeting of PDE4 isoforms. The molecular basis of such

anchoring in these transfected cells and in the range of cells in which these isoforms prove to be expressed natively remains to be determined. However, studies on various PDE4A isoforms expressed transiently in COS cells that have identified PDE4 isoforms targeted to particulate fractions have proved to reflect similar associations for the natively expressed forms [30,31,35].

Differences in the relative V_{max} have been noted for the cytosol-expressed components of various rodent PDE4A isoforms [30] as well as between the cytosol and particulate forms of various PDE4A species [30,31,37]. Here we observed, however, that whereas the relative V_{max} of PDE4B3 was slightly higher than that of the other long form, PDE4B1, the maximal catalytic activity of the short form, PDE4B2, was considerably (approx. 4-fold) greater (Table 2). A similar situation has been demonstrated for the rodent short-form PDE4A species RD1 (RNPDE4A1A; GenBank accession number M26715), which has a much higher activity (5-fold) than that of the various long forms [30]. One suggestion proposed [6,35] to account for such observations is the occurrence of an inhibitory domain within the N-terminal region. As the short-form splice variants lack the first conserved region (UCR1) then there is the possibility that this PDE4-specific region might be involved in regulating enzyme activity. Consistent with the notion that changes in this region can alter catalytic activity is the demonstration [24,39,40] that the protein kinase A-mediated phosphorylation of the PDE4D3 isoform, which occurs at Ser-54, located within the UCR1 region, leads to enzyme activation. The particulate-associated forms of both PDE4B1 and PDE4B2 have maximal catalytic activities that are approx. 60 % lower than the cytosolic components, whereas that of the particulate PDE4B3 form is similar to that of its cytosolic form (Table 2). The basis of this remains to be identified.

Rolipram has been shown to serve as a competitive inhibitor of the PDE4B2 isoform expressed in *S. cerevisiae* [22]. However, Dixon replots of such data indicated that a simple kinetic mechanism was not obeyed. Consistent with the notion that rolipram inhibits this enzyme through complex kinetics, we noted shallow dose–effect curves for rolipram inhibition with Hill coefficients that were less than unity (Table 2). Intriguingly, the particulate-associated component of the short PDE4B2 isoform demonstrated a markedly lower affinity for rolipram inhibition (approx. one-tenth) compared with its corresponding cytosolic component, with a similar but less pronounced effect (one-half to one-third) being seen for PDE4B3. However, this is not the first time that differences in sensitivity to inhibition by rolipram have been seen for the particulate- and cytosol-associated components of PDE4 isoforms, because, in contrast with the situation described here for PDE4B2, the particulate-associated component of the long form of human PDE4A, PDE46 (HSPDE4A4B) showed a much higher affinity for rolipram inhibition than the cytosol component [37]. It seems likely that either particulate association or the process leading to its occurrence caused a conformational change in the PDE4B2 isoform that affected its ability to interact with rolipram. Thus, as suggested before [57,58], rolipram might serve as a sensitive indicator for conformational changes induced in PDE4 isoforms.

Here we have described the molecular cloning of a novel long isoform of human PDE4B and its rat homologue. This demonstrates the same diversity of splice variants that occurs at the splice junction conserved in *D. melanogaster* [3]. The various PDE4B isoforms exhibit distinct N-terminal regions and, from expression studies done in COS7 cells, it seems that these regions can confer particular properties on the various isoforms. These, as also shown for PDE4A isoforms [30–32,34–36], seem to include the ability to undergo intracellular targeting and to effect changes in catalytic activity.

This work was supported by a grant from the Medical Research Council, a special equipment grant from the Wellcome Trust to MDH and a Wellcome Trust Travel Grant (M.D.H. and G.B.B.). G.B.B. was supported by grants from the Department of Veterans Affairs and the National Cancer Institute, U.S.A., as well as the core facilities for DNA sequencing and oligonucleotide synthesis of the Huntsman Cancer Institute supported by grant 5-PO-CA42014 from the National Cancer Institute.

REFERENCES

1 Beavo, J. A., Conti, M. and Heaslip, R. J. (1994) Mol. Pharmacol. **46**, 399–405
2 Beavo, J. A. (1995) Physiol. Rev. **75**, 725–748
3 Bolger, G. (1994) Cell. Signal. **6**, 851–859
4 Houslay, M. D. and Kilgour, E. (1990) in Cyclic Nucleotide Phosphodiesterases, vol. 2 (Beavo, J. A. and Houslay, M. D., eds.), pp. 185–226, John Wiley, Chichester
5 Manganiello, V. C., Murata, T., Taira, M., Belfrage, P. and Degerman, E. (1995) Arch. Biochem. Biophys. **322**, 1–13
6 Conti, M., Nemoz, G., Sette, C. and Vicini, E. (1995) Endocrin. Rev. **16**, 370–389
7 Conti, M., Swinnen, J. V., Tsikalas, K. E. and Jin, S. L. C. (1992) in Advances in Second Messenger and Phosphoprotein Research, vol. 25 (Strade, S. J. and Hikaka, H., eds.), pp. 87–99, Raven Press, New York
8 Thompson, W. J. (1991) Pharmacol. Ther. **51**, 13–33
9 Houslay, M. D., Sullivan, M. and Bolger, G. B. (1997) Adv. Pharmacol., in the press
10 Houslay, M. D. and Milligan, G. (1997) Trends Biochem. Sci. **22**, 217–224
11 Reeves, M. L., Leigh, B. K. and England, P. J. (1987) Biochem. J. **241**, 535–541
12 Dent, G. and Giembycz, M. A. (1995) Clin. Immunother. **3**, 423–437
13 Souness, J. E., Maslen, C., Webber, S., Foster, M., Raeburn, D., Palfreyman, M. N., Ashton, M. J. and Karlsson, J. A. (1995) Br. J. Pharmacol. **115**, 39–46
14 Schmiechen, R., Schneider, H. H. and Wachtel, H. (1990) Psychopharmacology **102**, 17–20
15 Thompson, W. J., Epstein, P. M. and Strada, S. J. (1979) Biochemistry **18**, 5228–5237
16 Marchmont, R. J. and Houslay, M. D. (1980) Biochem. J. **187**, 381–392
17 Marchmont, R. J., Ayad, S. R. and Houslay, M. D. (1981) Biochem. J. **195**, 645–652
18 Davis, R. L., Takayasu, H., Eberwine, M. and Myres, J. (1989) Proc. Natl. Acad. Sci. U.S.A. **86**, 3604–3608
19 Swinnen, J. V., Joseph, D. R. and Conti, M. (1989) Proc. Natl. Acad. Sci. U.S.A. **86**, 5325–5329
20 Bolger, G., Michaeli, T., Martins, T., St John, T., Steiner, B., Rodgers, L., Riggs, M., Wigler, M. and Ferguson, K. (1993) Mol. Cell. Biol. **13**, 6558–6571
21 Livi, G. P., Kmetz, P., McHale, M. M., Cieslinski, L. B., Sathe, G. M., Taylor, D. P., Davis, R. L., Torphy, T. J. and Balcarek, J. M. (1990) Mol. Cell. Biol. **10**, 2678–2686
22 McLaughlin, M. M., Cieslinski, L. B., Burman, M., Torphy, T. J. and Livi, G. P. (1993) J. Biol. Chem. **268**, 6470–6476
23 Engels, P., Sullivan, M., Muller, T. and Lubbert, H. (1995) FEBS Lett. **358**, 305–310
24 Alvarez, R., Sette, C., Yang, D., Eglen, R. M., Wilhelm, R., Shelton, E. R. and Conti, M. (1995) Mol. Pharmacol. **48**, 616–622
25 Baecker, P. A., Obernolte, R., Bach, C., Yee, C. and Shelton, E. R. (1994) Gene **138**, 253–256
26 Horton, Y. M., Sullivan, M. and Houslay, M. D. (1995) Biochem. J. **308**, 683–691
27 Milatovich, A., Bolger, G., Michaeli, T. and Francke, U. (1994) Somatic Cell Mol. Genet. **20**, 75–86
28 Szpirer, C., Szpirer, J., Riviere, M., Swinnen, J., Vicini, E. and Conti, M. (1995) Cytogenet. Cell Genet. **69**, 11–14
29 Horton, Y. M., Sullivan, M. and Houslay, M. D. (1995) Biochem. J. **312**, 991
30 Bolger, G., McPhee, I. and Houslay, M. D. (1996) J. Biol. Chem. **271**, 1065–1071
31 McPhee, I., Pooley, L., Lobban, M., Bolger, G. and Houslay, M. D. (1995) Biochem. J. **310**, 965–974
32 Scotland, G. and Houslay, M. D. (1995) Biochem. J. **308**, 673–681
33 Smith, K. J., Scotland, G., Beattie, J., Trayer, I. P. and Houslay, M. D. (1996) J. Biol. Chem. **271**, 16703–16711
34 Shakur, Y., Pryde, J. G. and Houslay, M. D. (1993) Biochem. J. **292**, 677–686
35 Shakur, Y., Wilson, M., Pooley, L., Lobban, M., Griffiths, S. L., Campbell, A. M., Beattie, J., Daly, C. and Houslay, M. D. (1995) Biochem. J. **306**, 801–809
36 Pooley, L., Shakur, Y., Rena, G. and Houslay, M. D. (1997) Biochem. J. **271**, 177–185
37 Huston, E., Pooley, L., Julien, J., Scotland, G., McPhee, I., Sullivan, M., Bolger, G. and Houslay, M. D. (1996) J. Biol. Chem. **271**, 31334–31344
38 O'Connell, J. C., McCallum, J. F., McPhee, I., Wakefield, J., Houslay, E. S., Wishart, W., Bolger, G., Frame, M. and Houslay, M. D. (1996) Biochem. J. **318**, 255–262
39 Sette, C. and Conti, M. (1996) J. Biol. Chem. **271**, 16526–16534
40 Sette, C., Iona, S. and Conti, M. (1994) J. Biol. Chem. **269**, 9245–9252
41 Colicelli, J., Birchmeir, C., Michaeli, T., O'Neill, K., Riggs, M. and Wigler, M. (1989) Proc. Natl. Acad. Sci. U.S.A. **86**, 3599–3603

42 Obernolte, R., Bhakta, S., Alvarez, R., Bach, C., Zuppan, P., Mulkins, M., Jarnagin, K. and Shelton, E. R. (1993) Gene **129**, 239–247
43 Short, J. M., Fernandez, J. M., Sorge, J. A. and Huse, W. D. (1988) Nucleic Acids Res. **16**, 7583–7600
44 Sambrook, J., Fritsch, E. F. and Maniatis, T. (1989) Molecular Cloning: A Laboratory Manual, Cold Spring Harbor Laboratory, Cold Spring Harbor, NY
45 Bolger, G. B., Rodgers, L. and Riggs, M. (1994) Gene **149**, 237–244
46 Lobban, M., Shakur, Y., Beattie, J. and Houslay, M. D. (1994) Biochem. J. **304**, 399–406
47 Thompson, W. J. and Appleman, M. M. (1971) Biochemistry **10**, 311–316
48 Rutten, W. J., Schoot, B. M. and Dupont, J. S. H. (1973) Biochim. Biophys. Acta **315**, 378–383
49 Bradford, M. M. (1976) Anal. Biochem. **72**, 248–254
50 Laemmli, U.K. (1970) Nature (London) **227**, 680–685
51 Conti, M., Iona, S., Cuomo, M., Swinnen, J. V., Odeh, J. and Svoboda, M. E. (1995) Biochemistry **34**, 7979–7987
52 Swinnen, J. V., Tsikalas, K. E. and Conti, M. (1991) J. Biol. Chem. **266**, 18370–18377
53 Monaco, L., Vicini, E. and Conti, M. (1994) J. Biol. Chem. **269**, 347–357
54 Davis, R. L. and Davidson, N. (1986) Mol. Cell. Biol. **6**, 1464–1470
55 Erdogan, S. and Houslay, M. D. (1997) Biochem. J. **321**, 165–175
56 Bolger, G. B., Erdogan, S., Jones, R. E., Loughney, K., Wilkinson, I., Farrell, C. and Houslay, M. D. (1997) Biochem. J. **328**, 539–548
57 Torphy, T. J., Stadel, J. M., Burman, M., Cieslinski, L. B., McLaughlin, M. M., White, J. R. and Livi, G. P. (1992) J. Biol. Chem. **267**, 1798–1804
58 Souness, J. E. and Rao, S. (1997) Cell. Signal. **9**, in the press

Received 15 May 1997/11 August 1997; accepted 26 August 1997